Science Translational Medicine
AAAS

www.sciencetranslationalmedicine.org/cgi/content/full/9/393/eaal1669/DC1

Supplementary Materials for

Ectopic calcification in pseudoxanthoma elasticum responds to inhibition of tissue-nonspecific alkaline phosphatase

Shira G. Ziegler,* Carlos R. Ferreira, Elena Gallo MacFarlane, Ryan C. Riddle, Ryan E. Tomlinson, Emily Y. Chew, Ludovic Martin, Chen-Ting Ma, Eduard Sergienko, Anthony B. Pinkerton, José Luis Millán, William A. Gahl, Harry C. Dietz*

*Corresponding author. Email: sgziegler@jhmi.edu (S.G.Z.); hdietz@jhmi.edu (H.C.D.)

Published 7 June 2017, *Sci. Transl. Med.* **9**, eaal1669 (2017)
DOI: 10.1126/scitranslmed.aal1669

The PDF file includes:

Other Supplementary Material for this manuscript includes the following:
(available at www.sciencetranslationalmedicine.org/cgi/content/full/9/393/eaal1669/DC1)

Table S5 (Microsoft Excel format). Individual-level data.

Materials and Methods

Subjects

Patients were enrolled in clinical protocol 76-HG-0238, "Natural History of Patients with Inborn Errors of Metabolism" (clinicaltrials.gov identifier NCT00369421), approved by the NHGRI Institutional Review Board. Written, informed consent was obtained.

Mice

Abcc6 knockout mice (*Abcc6*^{tm1Jfk}/J; termed *Abcc6*$^{-/-}$) were generously provided by Jouni Uitto at Thomas Jefferson University. *Enpp1*-ablated mice (*Enpp1*^{asj}/GrsrJ, stock number: 012810; termed *Enpp1*$^{-/-}$) and *Nt5e* knockout mice (*Nt5e* ^{tm1Lft}/J, stock number: 018986; termed *Nt5e*$^{-/-}$) were obtained from The Jackson Laboratory. The first sign of calcification in *Abcc6*$^{-/-}$ mice is in the fibrous capsule surrounding their vibrissae or whiskers on the muzzle *(17)*. While there is no human equivalent for this fibrous structure, its calcification has been well-established as an early biomarker for vascular calcification and can be monitored in vivo with micro-CT *(46)*. Therefore, all studies analyzed the vibrissae fibrous capsule calcification phenotype at 15 or 20 weeks of age since *Abcc6*$^{-/-}$ do not develop other signs of calcification without provocation until many months later, extending beyond the lifespan of *Enpp1*$^{-/-}$ mice. We found that *Nt5e*$^{-/-}$ mice did not develop fibrous capsule vibrissae calcification until 1 year of age. Therefore, *Abcc6* bred to *Nt5e* mice were analyzed at both 15 weeks and one year.

Abcc6$^{tm1a(EUCOMM)}$ embryonic stem cell lines with conditional potential were purchased from the European Conditional Mouse Mutagenesis Program. Embryonic stem cells were injected into an albino C57BL/6 blastocyst (B6N-*Tyr*$^{c-Brd}$/BrdCrCrl; Charles River) and chimeras were

generated. After germline transmission was confirmed, *Abcc6*$^{tm1a(EUCOMM)}$ mice were bred to B6.Cg-Tg(ACTFLPe)9205Dym/J (stock number: 005703) mice to generate *Abcc6*$^{tm1c(EUCOMM)}$ (termed *Abcc6*$^{flox/flox}$) mice. To knockout *Abcc6* in a cell-type and/or tissue-specific matter, these mice were bred to the following *Cre* expressing mouse lines, which were obtained from The Jackson Laboratory unless otherwise indicated: B6.C-Tg(CMV-cre)1Cgn/J (stock number: 006054; termed CMV-*Cre*), B6.Cg-Tg(Alb-cre)21Mgn/J (stock number: 003574; termed Alb-*Cre*), B6.Cg-Tg(Tagln-cre)1Her/J (stock number: 017491; termed SM22α-*Cre*), B6.FVB-Tg(Cdh5-cre)7Mlia/J (stock number: 006137; termed VE-cadherin-*Cre*), *Pax7*$^{tm1(cre)Mrc}$/J (stock number: 010530; termed Pax7-*Cre*), B6.Cg-Tg(Cdh16-cre)91Igr/J (stock number: 012237; termed Cdh16-*Cre*), Tg(Pdgfrb-Cre)^{35Vli} (a generous donation from Volkhard Lindner at Maine Medical Center; termed Pdgfrβ-*Cre*), B6.Cg-Tg(Fabp4-cre)1Rev/J (stock number: 005069; termed Fabp4-*Cre*), Ptprc$^{tm1(cre)Medv}$ (a generous donation from Joseph Mee at the University of Edinburgh; termed CD45-*Cre*), 129S4.Cg-Tg(Wnt1-cre)2Sor/J (stock number: 022137; termed Wnt1-*Cre*), and Tg(Cdx1-cre)23Kem (a generous donation from Jeremy Nathans at Johns Hopkins University School of Medicine; termed Cdx1-*Cre*). The B6.129(Cg)-*Gt(ROSA)26Sor*$^{tm4(ACTB-tdTomato,-EGFP)Luo}$/J (stock number: 007676, termed *Rosa*^{mTmG}) mouse line was employed to mark recombined cells.

For all crosses, litter size was normal, gender distribution of the progeny was balanced, and pups appeared healthy with the expected Mendelian patterns of gene transmission. Littermates were used as controls for analysis. All mice were maintained on a C57BL/6J background; mice derived from other strains or substrains were backcrossed onto C57BL/6J for at least five generations before proceeding with experimental crosses. Mice derived from other strains were

also checked for the SNP at position rs32756904 in exon 14 of *Abcc6* which has previously been shown to confound results when studying PXE in mice *(47).* All mice carried the non-disease associated allele in the homozygous state (G/G). Sequencing methods described below.

Mice were housed in a clean, specific pathogen-free facility with ventilated racks supplied with HEPA filtered, tempered, and humidified air and exhausted direct to the outside through the interstitial space above. Mice were given ad libitum access to standard global 19% protein extruded rodent diet (Envigo) unless otherwise indicated; see Drug treatments section below. Cages were supplied with reverse osmosis filtered hyperchlorinated water via an in-cage automatic watering system. Light was controlled by central timer providing 14 hours light/10 hours dark. The welfare of the mice was monitored daily by trained staff. All animal experiments were approved by the Johns Hopkins Animal Care and Use Committee and performed with strict adherence to their guidelines (protocol number MO15M88).

Mutation analysis

For human subjects, genomic DNA was isolated from leukocytes. For mice, genomic DNA was isolated from a piece of tail. All exon and intron-exon boundaries of *ABCC6*, *ENPP1*, or *NT5E* were amplified by polymerase chain reaction (PCR) using genomic DNA as a template. PCR was performed in a final volume of 10 µl containing 50 ng of genomic DNA, 1 µM of forward and reserve primers, and 5 µl of HotStart Master Mix (Qiagen). The PCR products were purified using ExoSap-IT for 45 minutes at 37 °C and sequenced in both directions using the same primers and the Big Dye terminator kit v3.1 (Applied Biosystems). Reactions were purified over G-50 Sephadex beads (Sigma-Aldrich). Linear amplification products were separated in an

automated capillary sequencer (ABI PRISM 3130xl Genetic Analyzer, Applied Biosystems). Sequences were analyzed with Sequencher software 4.8. Primer sequences available upon request.

Mouse genotyping

DNA was extracted from a piece of tail using an NaOH extraction *(48)*. PCR was performed in a final volume of 20 µl containing 2 µl of genomic DNA, 1 µM of each primer, and 10µl of REDTaq ReadyMix PCR Reaction Mix (Sigma-Aldrich). PCR products were then run on a 1.5% ethidium bromide-containing agarose gel and visualized under UV light. Primer sequences available upon request.

Cell culture

Primary dermal fibroblasts were cultured from a 3 or 4 mm forearm punch-biopsy specimen of skin, obtained from each patient, and grown in Dulbecco's modified Eagle's medium (Gibco) containing 10% fetal bovine serum (Sigma-Aldrich, Lot 15C177), 1 mM L-glutamine (Life Technologies), and 1% penicillin-streptomycin (Gibco), as previously described. Cells were fed twice a week and split 1:2 at confluence.

Osteogenic assay

A modified protocol for in vitro calcification was used for fibroblasts. Cells were grown until confluent and were treated with 0.1 µM dexamethasone (Sigma-Aldrich), 50 µM ascorbic acid-2-phosphate (Sigma-Aldrich), and 10 mM β-glycerophosphate (Sigma-Aldrich) in α-Minimal Essential Medium (Corning; termed αMEM) supplemented with 10% fetal bovine serum (Sigma-

Aldrich, Lot 15C177) and 1% penicillin-streptomycin (termed osteogenic media) for 21 days, with replenishment of the medium every 4 or 5 days. On day 21, cells were washed with phosphate-buffered saline (Gibco) and fixed in 10% formalin (Fisher Scientific) for 10 minutes. After washing with water, a solution of 2% alizarin red S (Sigma-Aldrich), pH 4.2, was used to stain calcium phosphate crystals. Bright field images of cells were obtained using a Nikon 80i with a color camera and a 10x objective and the NIS Elements software (Nikon). After imaging, to semi-quantify the staining, cells were incubated with 10% warm acetic acid for 30 minutes at room temperature. Cells were then scrapped down and spun at 16,000 g for 15 minutes. Supernatant was quantified at 405 nm on a spectrophotometer.

ENPP1, TNAP, and CD73 enzyme assays

Cells were seeded in 6-well plates and grown until confluent for five days. To measure ENPP1 enzyme activity, cells were lysed in 100 mM Tris-HCl (pH 9.0), 500 mM NaCl, 5 mM $MgCl_2$, and 0.05% Triton X-100 and scraped into microcentrifuge tubes and kept on ice. Cell suspensions were spun at 12,000 g for 5 minutes. A 50 µl aliquot of the supernatant was added to a clear-bottom 96-well plate and the reaction with initiated upon adding 50 µl of 1mM para-nitrophenol-thymidine monophosphate (pNP-TMP; Sigma-Aldrich).

For TNAP enzyme activity assays, cells were first stimulated with osteogenic media for five days. Measurement of TNAP was performed with the use of the StemTAG Alkaline Phosphatase Activity Assay kit (Cell BioLabs). Briefly, cells were washed with phosphate-buffered saline (Gibco) and then lysed and scraped down in Cell Lysis Buffer (Cell BioLabs). Cell suspensions were spun at 12,000 g for 5 minutes. A 50 µl aliquot of supernatant was added

to a clear-bottom 96-well plate and the reaction was initiated by adding 50 µl of StemTAG AP Activity Assay Substrate (Cell BioLabs).

Both ENPP1 and TNAP assays relied on the production of p-nitrophenol (pNP) to quantify enzymatic activity, as determined by absorption at 405 nm, and normalized to micrograms of protein (as quantified by a bicinchoninic acid assay; Pierce) over time (measured in minutes).

To measure CD73 enzyme activity, cells were washed with 2 mM magnesium chloride, 120 mM sodium chloride, 5 mM potassium chloride, 10 mM glucose, and 20 mM HEPES. Incubation buffer, consisting of the wash solution supplemented with 2 mM AMP, was added, and cells were incubated at 37 °C for 10 min. An aliquot of the supernatant was removed and inorganic phosphate was measured with the SensoLyte MG Phosphate Assay Kit (AnaSpec) according to the manufacturer's instructions. Inorganic phosphate measurements were normalized to micrograms of protein (as quantified by a bicinchoninic acid assay; Pierce).

Expression studies

RNA was isolated from cultured fibroblasts or solid organs with Trizol (Life Technologies) and the RNeasy kit (Qiagen). Solid organs were first homogenized with the MP shaker. RNA concentration and purity were measured on a Nanodrop ND-1000. First strand cDNA was synthesized using the high capacity RNA-to-cDNA kit (Life Technologies). Quantitative PCR was performed utilizing 1 µg cDNA, TaqMan gene expression master mix reagents, and probes specific for human *ENPP1, NT5E, ALPL,* and *ACTB* and mouse *Abcc6* and *Gapdh* (Life

Technologies) on a QuantStudio 7 (Life Technologies) using the $2^{-\Delta\Delta CT}$ method for relative gene expression.

Histology and immunofluorescence

Adult mice were humanely sacrificed via inhalation overdose of 2-Bromo-2-chloro-1,1,1-trifluoroethane (Sigma-Aldrich). Mice underwent immediate laparotomy, inferior vena cava transection, and phosphate-buffered saline was infused through the left ventricle to flush out the blood. Organs of interest were then excised. Organs were fixed in 4% PFA overnight at 4 °C before being subjected to dehydration with sequentially increasing concentrations of sucrose (10%, 20%, and 30% sucrose in phosphate-buffered saline) for 12 hours at 4 °C. Organs were then immersed in optimal cutting temperature compound (VWR Scientific) and slowly frozen over a liquid nitrogen bath. Ten µm sections were cut on a cryostat and placed on SuperFrost slides.

To visualize the location of calcification in the fibrous capsule of the vibrissae, 10 µm muzzle sections were stained with 2% alizarin red S (Sigma-Aldrich). Histological slides were then dehydrated in acetone and cleared in xylene before mounting with a synthetic mounting medium and imaged on a Nikon 80i with a color camera and a 10x objective with NIS Elements software (Nikon).

Immunofluorescent slides were washed with phosphate-buffered saline before being sealed with Hardset VectaShield containing DAPI (H-1500) and imaged on a Zeiss LSM 780 confocal microscope. To test for tissue and cell specificity of *Cre*-mediated recombination, all *Cre* mouse

lines were bred to a *Rosa*^{mTmG} reporter; expression of membrane green florescent protein indicates recombination. Endogenous expression of tdTomato and green florescent protein were imaged. To quantify the extent of mosaic recombination in the liver, the number of green hepatocytes was counted in three separate fields of view across three different *Rosa*^{mTmG};Wnt1-*Cre* adult mice.

Drug treatments

The development and characterization of the uncompetitive TNAP-specific inhibitor compound SBI-425 (PCT WO 2013126608; Preparation of pyridinylsulfonamide derivatives for use as TNAP inhibitors) was published previously *(21, 23)*. SBI-425 only binds to the enzyme in the presence of the substrate to form a three-way complex (inhibitor-enzyme-substrate) that effectively inhibits the enzyme. The inhibition is reversible upon dilution of the complex. Unlike bisphosphonates, SBI-425 does not bind to mineral where it could concentrate and provoke crystal toxicity. For the in vitro experiments, 10 μM SBI-425 (dissolved in 100% DMSO) or DMSO-control was added to the culture every time the medium was changed during the duration of the 21 day experiment.

Mouse chow was formulated with SBI-425 (30 mg/kg/day) or etidronate (240 mg/kg/day; TCI America), assuming a 20 g mouse who consumes 2 to 5 g of food/day. For SBI-425, the drug was crushed with mortar and pestle and added to powdered feed and vigorously mixed (300 mg of SBI-425 in 1 kg of powdered feed; LabDiet). For etidronate, custom-dyed food pellets were made after incorporation of etidronate into the feed (960 mg of etidronate in 1 kg of feed;

LabDiet). Control diet had the same standard base formulation as the drug-supplemented diets (LabDiet 5001).

Micro-CT imaging and analysis

All mice were imaged on a SPECT/CT (Gamma Medica X-SPECT) small animal machine. For the *Abcc6* and *Enpp1* genetic crosses, mice were analyzed at 15 weeks of age; for the *Abcc6* and *Nt5e* genetic crosses, mice were analyzed at 15 weeks and one year. For the *Abcc6*$^{flox/flox}$ mouse crosses, mice were analyzed at 20 weeks of age and one year. For the treatment trial, mice were scanned at six weeks of age (baseline analysis before initiation of treatment) and at 20 weeks of age (final analysis after 14 weeks on treatment).

Mice were anesthetized with continuous isoflurane during the acquisition of the micro-CT scans. Images were reconstructed and analyzed with ImageJ (NIH). Briefly, a Z-stack was created to encompass the entire region of pathological calcification (rostrally, from the tip of the nose to caudally, the zygomatic arch). To quantify this calcification, a threshold was manually determined to calculate the total area of ectopic calcification, excluding the radiodense nasal bones and sinuses. For the treatment trial, data are an average of micro-CT analysis by six masked observers.

Mouse plasma PPi assay

Adult mice were humanely sacrificed with inhalation overdose of 2-Bromo-2-chloro-1,1,1-trifluoroethane (Sigma-Aldrich). Mice underwent immediate laparotomy and blood was obtained from the inferior vena cava and collected directly into EDTA-coated microcontainers

(BD). Samples were placed on ice and spun at 20,000 g for 5 minutes at 4 °C within 5 minutes after sample collection. Plasma was placed onto a centrifugal filter (Ultrafree-MC UFC30VV00, Millipore) and spun again at 20,000 g for 5 minutes at 4 °C. Filtrate was collected and stored at -80 °C until further processing.

Detection of PPi relied on an enzymatic method to detect an ATP sulfurylase-catalyzed reaction and was modified from a previously published method *(49)*. Briefly, 10 µl of plasma sample or known PPi standard (ranging from 0.05 µM to 10 µM; Sigma-Aldrich) was added to 40 µl of assay mixture containing 20 µM adenosine 5' phosphosulfate sodium salt (Sigma-Aldrich), 25 µM $MgCl_2$, 12.5 mM HEPES with or without 1 U/ml ATP sulfurylase (New England BioLabs). The mixture was incubated at 37 °C for 30 minutes and heat-inactivated at 90 °C for 10 minutes. After centrifugation at 20,000 g for 5 minutes at 4 °C, 10 µl of supernatant was transferred in duplicate to a 96-well white-bottom plate. One-hundred µl of CellTiter-Glo 2.0 (diluted 1:5, Promega) was added to every well. Luminescence was measured after a 10-minute room temperature incubation in the dark. To generate a calibration curve, the luminescent signals were calculated by subtracting the blank signals (reaction without ATP sulfurylase) from the assay signals (reaction with ATP sulfurylase); the subtracted values were plotted against the PPi standards by a weighed least-squares linear regression method. Samples with noticeable hemolysis were excluded from analysis because of red blood cell contamination.

Calcium phosphate quantification

Adult mice were humanely sacrificed with inhalation overdose of 2-Bromo-2-chloro-1,1,1-trifluoroethane (Sigma-Aldrich). Mice underwent immediate laparotomy, inferior vena cava

transection, and phosphate-buffered saline was infused through the left ventricle to flush out the blood. The muzzle was dissected from the underlying nasal bones and bisected. Half of the muzzle was fixed in 10% formalin (Fisher Scientific) and frozen at -80 °C. The muzzle was then freeze-dried with a lyophilizer and weighed. The tissue was physically macerated before homogenizing with a bead homogenizer (MP) for 15 minutes at 4 °C. Tissue was then soaked overnight in 10% formic acid (Sigma-Aldrich). Samples were spun at 16,000 g for 5 minutes before 10 µl of the supernatant was used in a Calcium Quantification Assay (BioVision), as per manufacturer's instructions. Absorbance readings at 575 nm were normalized to tissue weight in grams.

Mouse plasma alkaline phosphatase analysis

At the conclusion of the treatment trial, mice were euthanized with inhalation overdose of 2-Bromo-2-chloro-1,1,1-trifluoroethane before collecting blood by cardiac puncture with a 21 gauge needle. Blood was collected in lithium-heparin-coated microcontainers (BD) for alkaline phosphatase analysis. Blood was spun at 150 g for 15 minutes at 4 °C and supernatant was collected and stored at -80 °C until assays were performed. Residual alkaline phosphatase levels were assayed as previously described *(50)*. Briefly, plasma samples were thawed on ice and spun at 2,400 g for 10 minutes. The plasma samples were mixed with substrates in buffer in 3:1 volume ratio to initiate the reaction in a 1536-well clear-bottom assay plate, with 1 mM $MgCl_2$, 50 µM $ZnCl_2$, 1 mM pNPP, and 100 mM diethanolamine buffer at pH 9.8. Ten µM of SBI-425 was spiked in control treatment plasma samples to determine non-TNAP phosphatase activity levels. Samples were read kinetically for an hour on the PHERAstar FS plate reader at 380 nm, to detect amount of pNP produced.

Bone microarchitecture and integrity studies

At the same time of sacrifice, the femur and tibia were dissected out en bloc and muscles and tendons were carefully removed. The bones were fixed in 4% PFA or stored at -20 °C until ex vivo analyses were performed. High resolution images of the mouse femur were acquired using a desktop micro-tomographic imaging system (Skyscan 1172, Bruker) in accordance with the recommendations of the American Society for Bone and Mineral Research (ASBMR) *(51).* Bones were scanned at 65 keV and 200 mA using a 0.5 mm aluminum filter with an isotropic voxel size of 10 µm. In the femur, trabecular bone parameters were assessed in the 500 µm proximal to the growth plate and extending for 2 mm (200 CT slices). Cortical bone structure was assessed 5 mm proximal to the growth plate and extending for 500 µm. Following this, fixed bones were embedded in resin and cut with on a macrotome; slides were stained with trichrome solutions. Images of slides were captured on a Nikon 80i with a color camera and a 40x objection using NIS Elements software (Nikon). Frozen femora were subjected to three point bending on a Bose Electroforce 3100. Force-displacement data were analyzed using a custom MATLAB script.

FIGURES

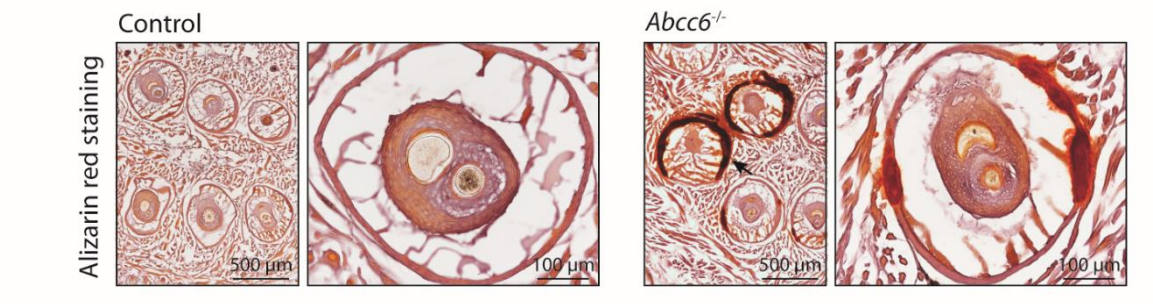

Fig. S1. Location of calcification in the fibrous capsule surrounding the vibrissae. Arrow indicates calcification, as demonstrated by alizarin red staining.

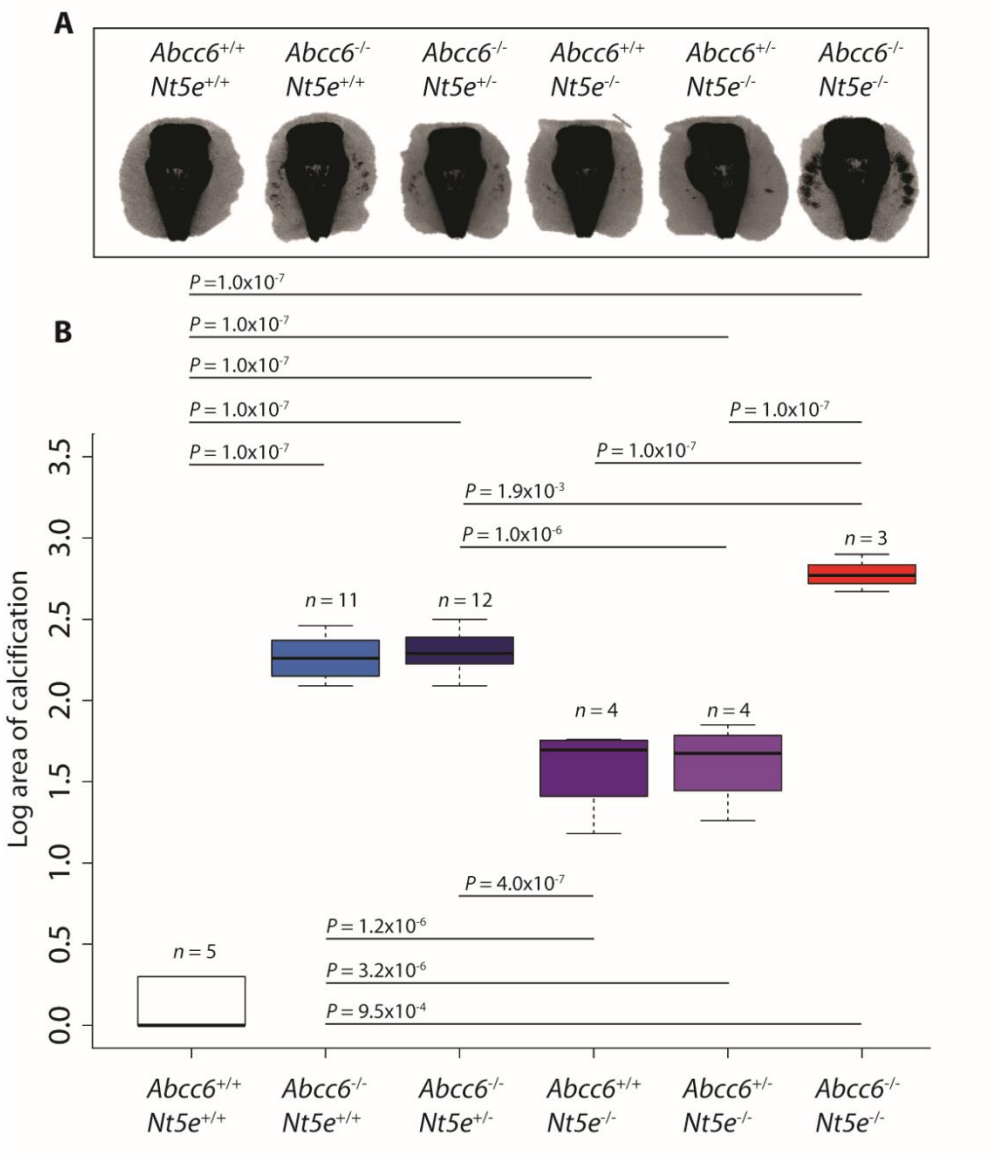

Fig. S2. Demonstration of genetic interaction between *Abcc6* and *Nt5e* mice when aged to 1 year. (**A**) Micro-CT scans of the muzzle to evaluate the extent of vibrissae fibrous capsule calcification were obtained at 1 year of age. (**B**) Quantification of ectopic calcification from micro-CT images. A two-way ANOVA with a Tukey's honest significance difference post-hoc analysis was performed. Two-way ANOVA: *Abcc6* effect: $P = 2.2\text{x}10^{-16}$, *Nt5e* effect: $P = 1.7\text{x}10^{-13}$, interaction effect: $P = 5.8\text{x}10^{-7}$. *P*-values of post-hoc comparisons are indicated in the figure.

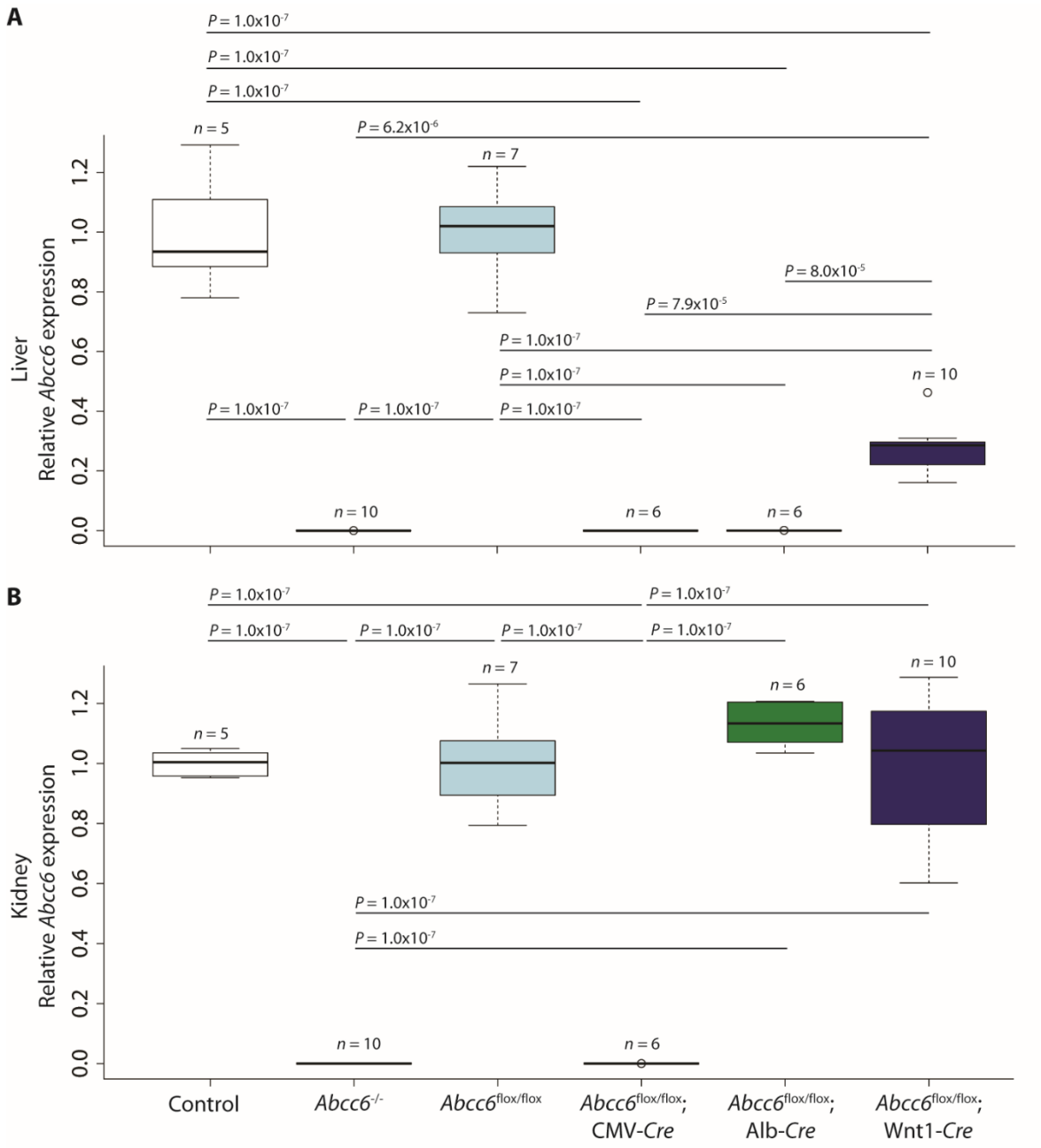

Fig. S3. Demonstration of efficient liver-specific deletion of *Abcc6* in mice. Expression of *Abcc6* in the liver (**A**) and kidney (**B**) of control, *Abcc6*$^{-/-}$, and *Cre*-targeted *Abcc6*$^{flox/flox}$ mice. A one-way ANOVA with a Tukey's honest significance difference post-hoc analysis was performed. One-way ANOVA: (A) $P = 2.2x10^{-16}$; (B) $P = 2.2x10^{-16}$. *P*-values of post-hoc comparisons are indicated in the figure.

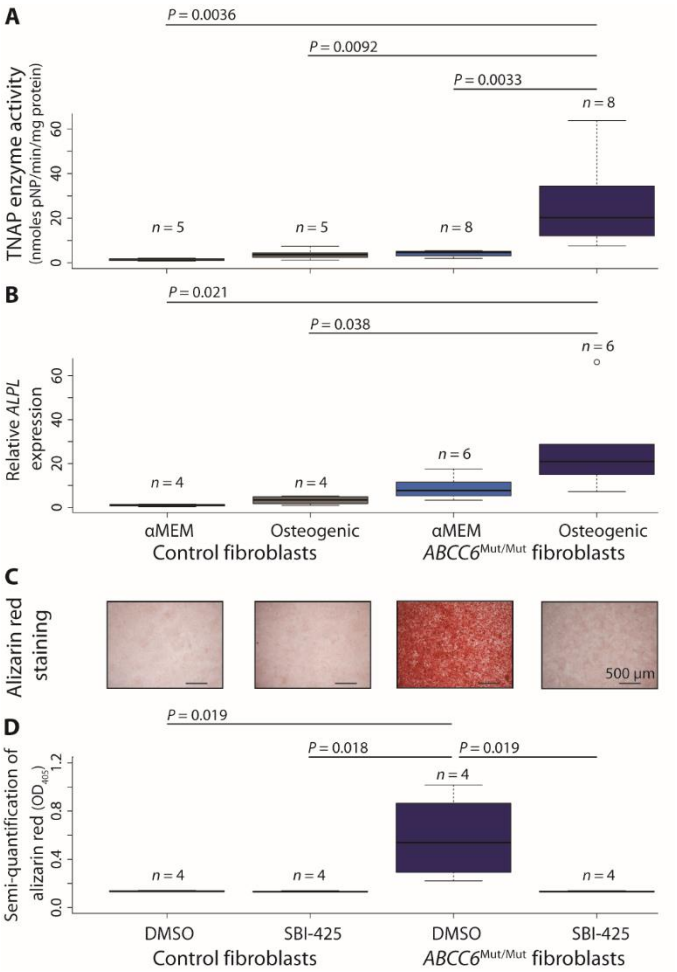

Fig. S4. Primary dermal fibroblasts derived from patients with biallelic mutations in *ABCC6* show TNAP-dependent in vitro calcification. (**A** and **B**) TNAP enzyme activity and gene (*ALPL*) expression in control and *ABCC6*$^{Mut/Mut}$ fibroblasts with and without osteogenic stimulation. (**C** and **D**) Calcification of *ABCC6*$^{Mut/Mut}$ fibroblasts is abrogated upon treatment with the TNAP inhibitor, SBI-425. (A to D) A two-way ANOVA with a Tukey's honest significance difference post-hoc analysis was performed. Two-way ANOVA: (A) genotype effect: $P = 0.010$, treatment effect: $P = 0.0029$, interaction effect: $P = 0.039$; (B) genotype effect: $P = 0.012$, treatment effect: $P = 0.048$, interaction effect: $P = 0.18$; (D) genotype effect: $P = 0.029$, treatment effect: $P = 0.028$, interaction effect: $P = 0.029$. *P*-values of post-hoc comparisons are indicated in the figure.

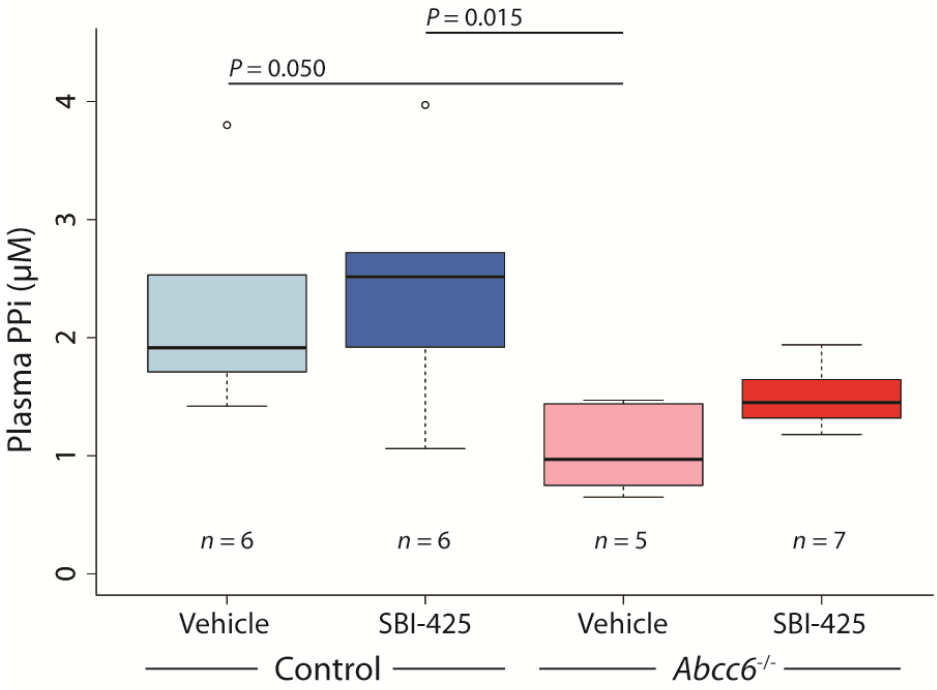

Fig. S5. TNAP inhibition does not alter circulating PPi concentration in mice.

Quantification of PPi concentrations in control and *Abcc6*$^{-/-}$ mice treated with vehicle or the TNAP inhibitor SBI-425. A two-way ANOVA with a Tukey's honest significance difference post-hoc analysis was performed. Two-way ANOVA, genotype effect: $P = 0.0017$, treatment effect: $P = 0.24$, interaction effect: $P = 0.72$. *P*-values of post-hoc comparisons are indicated in the figure.

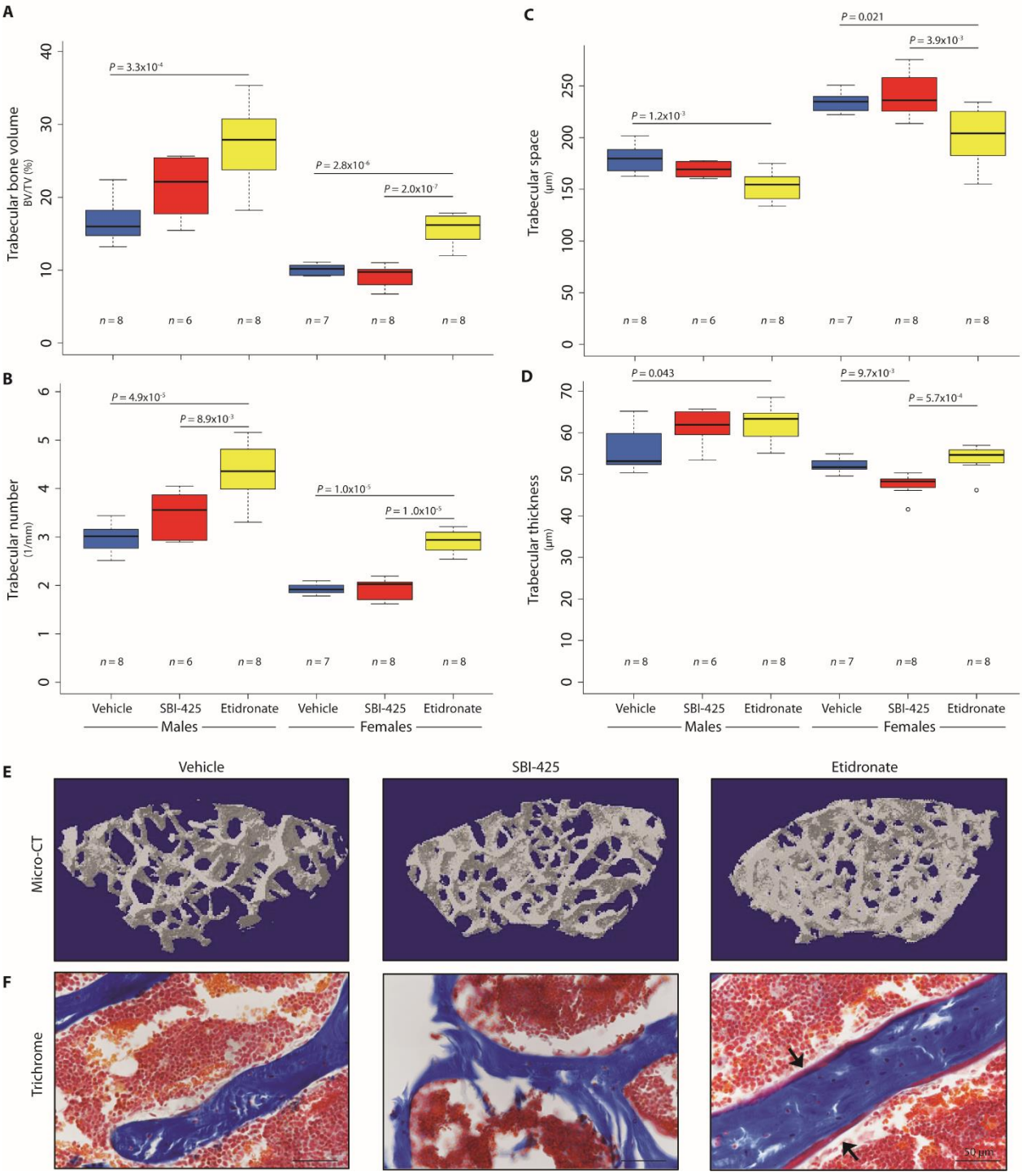

Fig. S6. TNAP inhibition had no negative effects on bone microarchitecture or mineralization in a PXE mouse model. Quantification of trabecular bone volume (**A**), number (**B**)**,** space (**C**), and thickness (**D**) in vehicle-, SBI-425-, and etidronate- treated mice. Since there

was no effect of genotype in any of the trabecular bone parameters, genotype was collapsed to evaluate for differences across treatment groups within each sex with a one-way ANOVA and a Tukey's honest significance difference post-hoc test. *P*-values of post-hoc comparisons are indicated in the figure. Representative images from micro-CT scans (**E**) and trichrome staining of the distal femur (**F**). Arrows point to osteoid.

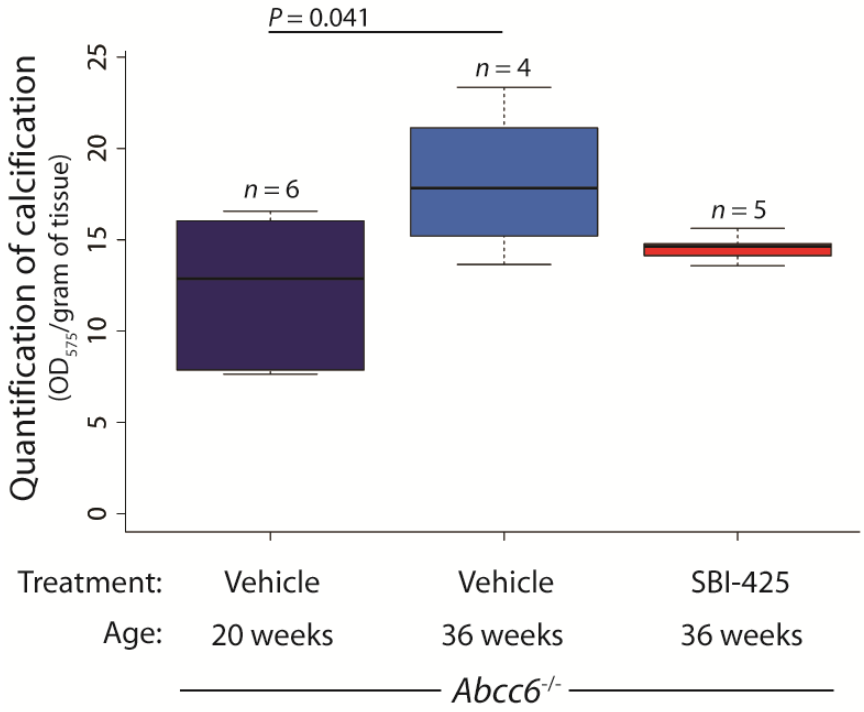

Fig. S7. TNAP inhibition prevents progression of established calcification in a PXE mouse model. *Abcc6*$^{-/-}$ mice were aged to 20 weeks and then treated with either vehicle or SBI-425 for 16 weeks. The calcium phosphate precipitate was quantified at the specified time point. A one-way ANOVA with a Tukey's honest significance difference post-hoc analysis was performed. One-way ANOVA: $P = 0.050$. P-values of post-hoc comparisons are indicated in the figure.

Table S1. List of patient mutations in *ABCC6*, *ENPP1*, and *NT5E*.

	Allele 1	Allele 2
ABCC6$^{Mut/Mut}$		
Patient I	c.1552C>T (p.Arg518*)	c.951C>A (p.Ser317Arg)
Patient II	c.3940C>T (p.Arg1314Trp)	c.3940C>T (p.Arg1314Trp)
Patient III	c.2861_2866del6 (p.Phe954_Leu955del)	Deletion of exons 2-31
Patient IV	c.3940C>T (p.Arg1314Trp)	c.3940C>T (p.Arg1314Trp)
Patient V	c.3940C>T (p.Arg1314Trp)	c.3940C>T (p.Arg1314Trp)
Patient VI	c.3940C>T (p.Arg1314Trp)	c.3940C>T (p.Arg1314Trp)
Patient VII	c.3421C>T (p.Arg1141*)	c.3490C>T (p.Arg1164*)
Patient VIII	c.999_1403del (deletion of exon 10)	c.2278C>T (p.Arg760Trp)
ENPP1$^{Mut/Mut}$		
Patient I	c.2596G>A (p.Glu866Lys)	c.803A>G (p.Tyr268Cys)
Patient II	c.2713_2717delAAAGA (p.Lys905fs*15)	c.1441C>T (p. Arg481Trp)
Patient III	c.2735T>C (p.Leu91Ser)	delIVS5_IVS6 (3.4kb deletion of exon 6)
Patient IV	c.1438T>C (p.Cys480Arg)	c.2414G>T (p.Gly805Val)
NT5E$^{Mut/Mut}$		
Patient I	c.662C>A (p.S221*)	c.662C>A (p.S221*)
Patient II	c.662C>A (p.S221*)	c.1609dupA (p.V537fs*7)
Patient III	c.1237C>T (p.Arg413*)	c.1237C>T (p.Arg413*)

Table S2. Number of calcified mice at 20 weeks and 1 year of age.

	Abcc6$^{flox/flox}$; CMV-*Cre*	*Abcc6*$^{flox/flox}$; Alb-*Cre*	*Abcc6*$^{flox/flox}$; SM22α-*Cre*	*Abcc6*$^{flox/flox}$; VE-cad-*Cre*	*Abcc6*$^{flox/flox}$; Pax7-*Cre*	*Abcc6*$^{flox/flox}$; Cdh16-*Cre*	*Abcc6*$^{flox/flox}$; Pdgfrβ-*Cre*	*Abcc6*$^{flox/flox}$; Fabp4-*Cre*	*Abcc6*$^{flox/flox}$; CD45-*Cre*	*Abcc6*$^{flox/flox}$; Wnt1-*Cre*
	Constitutive	Liver	Vascular smooth muscle	Vascular endothelium	Skeletal muscle	Renal tubular cells	Pericytes	Adipocytes	Bone marrow cells	Fibrous capsule cells
20 weeks										
Penetrance	12/12	0/13	0/10	0/9	0/16	0/23	0/10	0/11	0/10	1/22
Percent	100%	0%	0%	0%	0%	0%	0%	0%	0%	4.5%
1 year										
Penetrance	7/7	11/11	0/8	0/8	0/6	0/23	0/10	0/9	0/9	8/24
Percent	100%	100%	0%	0%	0%	0%	0%	0%	0%	33.3%

Table S3. Cortical bone microarchitecture. Treatment with SBI-425 or etidronate did not affect cortical bone microarchitecture. TMD = total mineral density; BA/TA = bone area/total area; pMOI = polar moment of inertia. Data presented as mean ± standard deviation.

	TMD (g/cm^3)	Tissue area (mm^2)	Bone area (mm^2)	BA/TA (%)	Marrow area (mm^2)	Cortical thickness (μm)	pMOI (mm^4)
Males							
Vehicle	1.22 ± 0.02	1.61 ± 0.13	0.84 ± 0.06	52.21 ± 1.29	0.77 ± 0.07	184.87 ± 11.00	0.34 ± 0.05
SBI-425	1.22 ± 0.02	1.82 ± 0.23	0.94 ± 0.12	51.49 ± 1.58	0.88 ± 0.12	178.10 ± 13.00	0.43 ± 0.10
Etidronate	1.22 ± 0.02	1.81 ± 0.26	0.95 ± 0.14	52.50 ± 1.83	0.86 ± 0.13	178.69 ± 8.64	0.43 ± 0.12
Females							
Vehicle	1.24 ± 0.04	1.52 ± 0.07	0.81 ± 0.03	53.05 ± 1.73	0.71 ± 0.05	195.15 ± 8.18	0.30 ± 0.03
SBI-425	1.21 ± 0.04	1.51 ± 0.07	0.79 ± 0.05	51.99 ± 2.34	0.73 ± 0.06	185.42 ± 6.43	0.29 ± 0.03
Etidronate	1.21 ± 0.03	1.52 ± 0.09	0.81 ± 0.07	53.27 ± 2.57	0.71 ± 0.04	185.61 ± 15.17	0.30 ± 0.05

Table S4. Cortical bone strength. Treatment with SBI-425 or etidronate did not affect cortical bone strength as evidenced by mechanical testing. Data presented as mean ± standard deviation.

	Ultimate Moment (Nmm)	Bending rigidity (Nmm^2)	Ultimate stress (MPa)	Young's modulus (MPa)	Ultimate displacement (mm)	Toughness (J/mm^3)
Males						
Vehicle	24.31 ± 4.21	556.14 ± 83.37	64.10 ± 4.61	2649.59 ± 584.13	0.49 ± 0.11	4.47 ± 1.18
SBI-425	27.32 ± 4.62	636.96 ± 210.14	59.88 ± 7.13	2285.95 ± 662.57	0.43 ± 0.14	4.45 ± 2.03
Etidronate	26.34 ± 4.65	670.84 ± 113.70	60.18 ± 5.24	2624.95 ± 294.17	0.53 ± 0.16	5.03 ± 2.01
Females						
Vehicle	24.40 ± 1.56	637.74 ± 43.43	74.74 ± 9.58	3419.77 ± 595.07	0.53 ± 0.28	5.76 ± 2.93
SBI-425	23.80 ± 1.25	590.60 ± 86.27	74.71 ± 5.89	3256.18 ± 464.60	0.47 ± 0.10	5.19 ± 1.12
Etidronate	24.43 ± 3.34	532.41 ± 126.29	73.98 ± 5.60	2863.08 ± 890.42	0.50 ± 0.14	5.74 ± 1.43